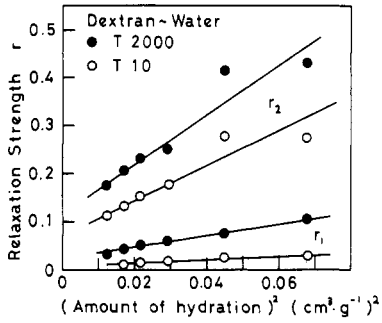

Figure 5. Relationship between relaxation strength, r, and amount of hydration: (●) dextran T-2000; (○) dextran T-10.

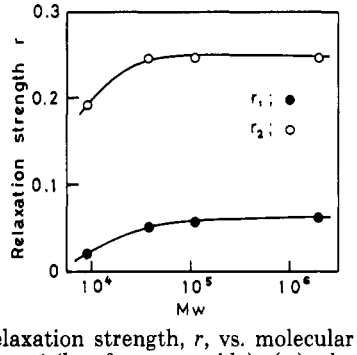

Figure 6. Relaxation strength, r, vs. molecular weight: (●) relaxation process 1 (low-frequency side); (○) relaxation process 2 (high-frequency side).

polymer chain in such a way as to cause rearrangement of water molecules weakly interacting with the polymer chain. This rearrangement gives rise to the volume relaxation.

In analogy with Ono et al.,[16] we can derive eq 3, which relates the ultrasonic relaxation strength r to the volume change ΔV in the segmental motion. ρ is the density, u

$$r \simeq \frac{2\mu_{max}}{\pi} = \frac{\rho u^2}{M_s RT} CgH(x)(\Delta \bar{V})^2 \qquad (3)$$

is the sound velocity, M_s is the molecular weight of the segment, R and T are the ideal gas constant and absolute temperature, respectively, the function $H(x)$ is determined from the type of molecular motion, and g is the fraction of the segment associated with the motion in the polymer chain.

The $\rho u^2/T$ calculated from the experimental values of ρ and u is found to be almost independent of temperature. Assuming that $H(x)$ and M_s are independent of temperature yields the expectation of a linear correlation in the plots of r vs. $(\Delta V)^2$. We must also assume that ΔV can be substituted by the amount of hydration of dextran.

Figure 5 shows the relationship between the relaxation strength and square of the amount of hydration. Clearly, the linear correlation holds between them. Figure 6 shows the molecular weight dependence of relaxation strength. As is seen in Figure 6, the relaxation strengths are almost independent of molecular weight. This result is similar to that of hydration reported by Gekko and Noguchi.[15]

Thus, we have demonstrated that the ultrasonic relaxation processes observed in aqueous solutions of dextran are most likely associated with the exchange process of water molecules in the hydration sphere of the polymer.

References and Notes

(1) M. Wales, P. A. Marshall, and S. G. Weisberg, *J. Polym. Sci.*, **10**, 229–40 (1953).
(2) F. R. Senti, N. N. Hellman, N. H. Ludwig, G. E. Babcock, R. Tobin, C. A. Glass, and B. L. Lamberts, *J. Polym. Sci.*, **17**, 527–46 (1955).
(3) E. Antonini, L. Bellelli, M. R. Bruzzesi, A. Caputo, E. Chiancone, and A. Rossi-Fanelli, *Biopolymers*, **2**, 27–34 (1964).
(4) H. Nomura, S. Kato, and Y. Miyahara, *Mem. Fac. Eng. Nagoya Univ.*, **27**, 72–125 (1975).
(5) J. I. Dunber, A. M. North, R. A. Pethrick, and D. B. Steinhauer, *J. Polym. Sci.*, **15**, 263–77 (1977).
(6) S. A. Hawley and F. Dunn, *J. Chem. Phys.*, **50**, 3523–6 (1969).
(7) S. Kato, H. Nomura, and Y. Miyahara, *Polym. J.*, **11**, 455–61 (1979).
(8) W. J Gettins, P. L. Jobling, and E. Wyn-Jones, *J. Chem. Soc., Faraday Trans. 2*, 1246–52 (1978).
(9) D. A. MacInes and A. M. North, *Polymer*, **18**, 505–8 (1977).
(10) D. A. MacInes, *J. Polym. Sci.*, **15**, 657–74 (1974).
(11) D. Pugh and D. A. Jones, *Polymer*, **19**, 1008–14 (1978).
(12) W. H. Stockmayer and K. Matsuo, *Macromolecules*, **5**, 766–70 (1972).
(13) J. Lamb in "Physical Acoustics", Vol. II, Part A, W. P. Mason, Ed., Academic Press, New York, 1965, Chapter 4, pp 203–80.
(14) H. Nomura, S. Yamaguchi, and Y. Miyahara, *J. Appl. Polym. Sci.*, **8**, 2731–4 (1964).
(15) K. Gekko and H. Noguchi, *Biopolymers*, **10**, 1513–24 (1971).
(16) K. Ono, H. Shintani, O. Yano, and Y. Wada, *Polym. J.*, **5**, 164–75 (1973).
(17) W. Ludlow, E. Wyn-Jones, and J. Rassing, *Chem. Phys. Lett.*, **13**, 477–81 (1972).
(18) B. H. Zimm, *J. Chem. Phys.*, **24**, 269–78 (1956).

An Unusual Relaxation in Certain Copolymers of Ethylene and Propylene†

Howard W. Starkweather, Jr.

E. I. du Pont de Nemours and Co., Central Research and Development Department, Wilmington, Delaware 19898. *Received October 9, 1979*

ABSTRACT: In copolymers of ethylene and propylene made with vanadium-based catalysts and having relatively low E/P mole ratios, a secondary dynamic mechanical loss peak almost as large as that resulting from the glass transition was observed at −115 to −90 °C in experiments with a torsion pendulum. This phenomenon appears to be associated with dimethylene links and propylene reversals. The relaxation is not accompanied by a change in the coefficient of thermal expansion or the heat capacity and may be described in terms of a single relaxation time. It is seen in shear, but not in flexure. A similar polymer made with a titanium-based catalyst which does not contain reversed propylene units did not exhibit this relaxation.

Copolymers of ethylene and propylene constitute an important family of hydrocarbon elastomers. Terpolymers containing a diene monomer such as 1,4-hexadiene or ethylidenenorbornene as a cross-linking site are known as EPDM rubbers. A number of studies[1-6] have located the glass temperature, T_g, between −60 and −50 °C over a broad range of composition. There is a shallow minimum

† Contribution No. 2716.

0024-9297/80/2213-0892$01.00/0

Table I
Heat Capacity and Thermal Expansion

	sample					value expected from ref 7
	1	2	3	4	5	
catalyst type	V	V	V	V	Ti	
E/P mole ratio	1.3	1.9	2.6	3.6	1.3	
	DSC Data					
T_g, °C	−56	−56	−54	−52	−51	
ΔC_p, cal deg^{-1} g^{-1}	0.15	0.26	0.30	0.20	0.15	
ΔC_p, cal deg^{-1} mol^{-1} of chain atoms	2.6	4.3	4.8	3.1	2.6	2.7
	Thermal Expansion Data					
T_g, °C	−42	−42	−24	−37		
$10^4\alpha_l$, deg^{-1}	6.5	9.2	9.1	6.5		
$10^4\alpha_g$, deg^{-1}	2.0	2.3	2.4	2.8		2
$10^4\Delta\alpha$, deg^{-1}	4.5	6.9	6.7	3.7		
$\alpha_l T_g$	0.15	0.21	0.23	0.15		0.16
$\Delta_\alpha T_g$	0.10	0.16	0.17	0.09		0.11

in T_g near 50% ethylene and a smooth increase toward the T_g of atactic polypropylene as the ethylene content is decreased below 40 mol %. Above 80 mol % ethylene, the glass temperature is obscured by increasing levels of crystallinity.

It has been suggested[6] that the rise in T_g with increasing ethylene content may be due to enrichment of the propylene content in the amorphous regions following crystallization of some of the ethylene sequences. It has been reported[6] that copolymers containing more than 60–75 mol % ethylene have melting points above room temperature and that the melting point reaches T_g at 40 mol % ethylene.

The effect of the diene monomers on T_g is relatively small. Baldwin and Ver Strate[6] reported that ethylidenenorbornene increases T_g by only 0.8 °C/wt % diene.

Torsion Pendulum Studies. Four binary copolymers of ethylene and propylene made with a vanadium tetrachloride/diisobutylaluminum chloride catalyst were run on the Plastech torsion pendulum. The ethylene/propylene mole ratios as determined by carbon-13 NMR spectroscopy varied from 1.3 to 3.6. The logarithmic decrements are plotted in Figure 1. All of the polymers exhibited a large damping peak near −60 °C as expected from the literature data on T_g. However, the sample having an E/P ratio of 1.3 had an additional large peak at −115 °C, and a sample having an E/P ratio of 1.9 had a peak at −90 °C. At E/P ratios of 2.6 and 3.6, the second large peak was absent, and the small γ relaxation near −125 °C which is characteristic of polymers and copolymers of ethylene was revealed.

A similar pattern was found in a series of EPDM terpolymers containing about 6% 1,4-hexadiene by weight. As shown in Figure 2, polymers having E/P mole ratios of 2.0 and 2.9 exhibited a large secondary loss peak near −90 °C while only the small γ relaxation was seen at an E/P ratio of 3.9. Very large secondary loss peaks at −100 to −80 °C along with T_g peaks at −65 to −55 °C have also been observed in EPDM terpolymers containing ethylidenenorbornene and having relatively low E/P mole ratios.

A strikingly different situation obtained when a γ-titanium trichloride/triethylaluminum catalyst was used instead of the vanadium-based system. The titanium-based catalyst tends to produce isotactic propylene sequences without the propylene reversals which are common with the other system. Polymers having E/P mole ratios of 1.3 are compared in Figure 3. The polymer made with the titanium-based catalyst had no strong secondary loss peak, only the T_g peak at −45 °C and the small γ relaxation.

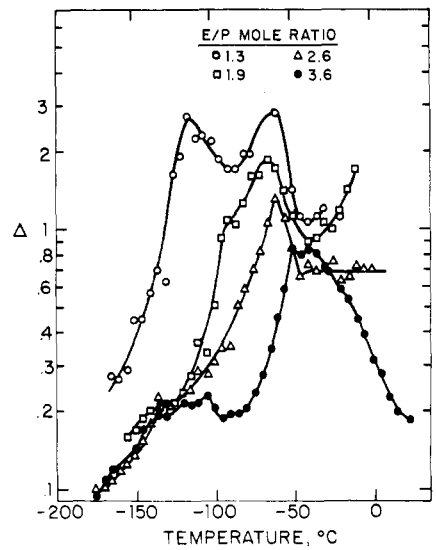

Figure 1. Internal friction of ethylene/propylene dipolymers.

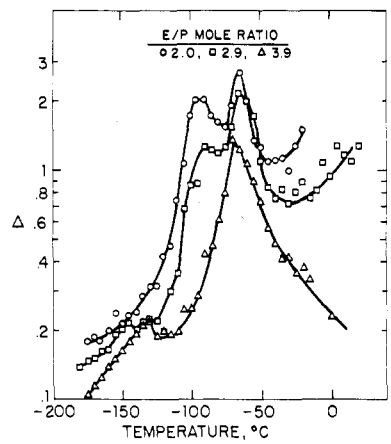

Figure 2. Internal friction of EPDM terpolymers containing 6% 1,4-hexadiene by weight.

Other Tests for the Glass Temperature. It is very unusual for a polymer to have two dynamic mechanical loss peaks as large as those presented here. It was thought that some of the samples might be blends of two materials, each with its own glass temperature.

Both the coefficient of thermal expansion and the heat capacity increase at the glass temperature, and empirical rules have been established for these increases.[7] The pertinent data for the ethylene/propylene dipolymers used

Table II
Data from Carbon-13 NMR Spectroscopy

	sample				
	1	2	3	4	5
catalyst type	V	V	V	V	Ti
mol % P[a]	44.0	33.8	27.8	21.9	43.8
E/P mol ratio by NMR[b]	1.3	1.9	2.6	3.6	1.3
no. of $(CH_2)_n$ sequences/100 monomer units					
$n = 1$	9.9	4.7	2.6	1.7	18.8
$n = 2$	5.6	2.2	1.3	0.4	nil
$n = 3$	7.3	4.1	2.2	1.5	10.0
$n = 4$	5.0	1.9	0.8	0.5	nil
$n = 5$ or more	16.1	20.9	21.0	17.8	8.8
av n[c]	3.5	4.9	6.2	8.1	3.6
propylene reversal ratio[d]	0.44	0.35	0.37	0.21	nil
no. of P_n sequences/100 monomer units					
$n = 1$	24.5	22.1	20.6	17.0	20.0
$n = 2$	9.5	7.0	4.5	6.4	12.5
no. of EPPE sequences/100 monomer units					
$^1/_2 f_P^2 \times 100$	9.68	5.71	3.86	2.40	9.59
av of $(CH_2)_1$ and P_2	9.7	5.85	3.55	2.45	15.6
no. of PEP sequences/100 monomer units					
$f_P^2(1 - f_P) \times 100$	10.84	7.56	3.75	3.75	10.78
sum of $(CH_2)_2$ and $(CH_2)_3$	12.9	6.3	3.5	1.9	10.0
χ[e]	0.776	0.634	0.437	0.376	1.19
$r_1 r_2$[f]	0.231	0.418	0.420	0.557	0.431

[a] $f_P \times 100$. [b] f. [c] (% P + 2 % E)/% P. [d] $N_2/(N_2 + N_3)$. [e] (% of propylenes in sequences of 2 or greater)/(% of isolated propylenes). [f] $1 + f(1 + \chi) - (1 + f)(1 + \chi)^{1/2}$.

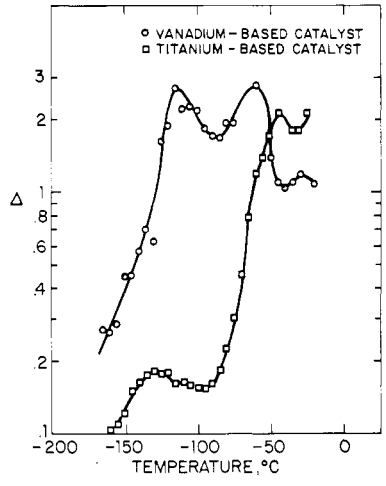

Figure 3. Internal friction of ethylene/propylene copolymers of mole ratio 1.3.

in the torsion pendulum experiments are given in Table I. Coefficients of linear thermal expansion were measured with the Du Pont thermomechanical analyzer and multiplied by 3 to get the volumetric coefficients reported in the table. Values of ΔC_p were measured by differential scanning calorimetry.

There were no significant changes in the coefficient of thermal expansion or the heat capacity associated with the relaxation near −90 °C. The DSC data are quite consistent with the dynamic mechanical loss peak near −60 °C. Values of T_g estimated from the thermal expansion data were somewhat higher and more variable. The thermal expansion behavior in this region was entirely consistent with that established in the literature for a wide variety of amorphous polymers.[7] The changes in heat capacity at the glass temperature for samples 1 and 5 were in line with the literature values, but other polymers tended to have larger increases in the heat capacity at T_g. In some cases, this was attributed to the onset of a first-order transition at temperatures not too far above T_g, which made it difficult to establish a good base line on the high-temperature side. It is also possible that the methyl side groups contribute to ΔC_p.

Clearly from these studies, the dynamic mechanical loss peak near −60 °C is associated with the glass temperature, and the loss peak near −90 °C is a secondary relaxation which involves little if any change in free volume.

Short Segment Structure. Since secondary relaxations are usually associated with small portions of a polymer molecule, a series of ethylene/propylene copolymers was examined by carbon-13 NMR spectroscopy, and the data were analyzed in terms of assignments reported in the literature.[8,9] The results of this study are presented in Table II. Samples 1–4 were examined with a Bruker HX 270 spectrometer at The Florida State University at a frequency of 67.95 MHz, and sample 5 was examined with a Bruker WH 90 spectrometer at a frequency of 22.63 MHz.

Interest centers on the various sequences of methylene units between branch points. It seems probable that the new low-temperature relaxation is associated with one of the short methylene sequences. Isolated methylenes are attributed to propylene sequences, and since they also occur in polypropylene, which does not have the relaxation near −90 °C, they are probably not the cause of that relaxation in the ethylene/propylene copolymers. Sequences of four or more methylenes have been associated with the γ relaxation which occurs near −125 °C in polyethylene, nylon, poly(tetramethylene terephthalate), and many other polymers.[10] In addition to being located at a lower temperature, the γ relaxation is much weaker than the −90 °C relaxation in the present copolymers, having a maximum logarithmic decrement of approximately 0.2.

By elimination, sequences of two or three methylene units between methyl branches are the most likely candidates for the −90 °C relaxation. Both of these structures arise from propylene–ethylene–propylene sequences. Even numbers of CH_2 units occur only as a result of propylene reversals during the polymerization. In principle, a sequence of two methylene units between methyl branches could result from a pair of propylene units with one reversed. However, carbon-13 enrichment studies by Brame

and Holmquist[11] indicated that most of these structures come from propylene-ethylene-propylene sequences. From the relative number of sequences of two and three methylene units, it is concluded that 30–40% of the propylene units are reversed in the copolymers made with a vanadium-based catalyst.

Reports in the literature indicate that sequences of two or four methylenes are common in ethylene/propylene copolymers made with the vanadium-based catalysts customarily used for the polymerization of EP rubber[8] but not in copolymers made from titanium-based catalysts which produce isotactic placements of the propylene units.[12] This is confirmed by a comparison of samples 1 and 5, which have the same ethylene/propylene ratio but were made by vanadium- and titanium-based catalysts, respectively. Sequences of two and four methylene units between branch points occur in sample 1 but not in sample 5. As the propylene content is reduced in samples 2–4, the concentration of these sequences is reduced and longer polymethylene segments predominate. Thus, there is good correlation between the concentration of dimethylene links between branch points and the strong secondary relaxation near −90 °C.

It appears that the placement of ethylene and propylene units in the copolymers is nearly random. The number of EPPE sequences per 100 monomer units should be $^1/_2 f_P^2 \times 100$, where f_P is the mole fraction of propylene units. It is seen in Table II that this is quite close to the average of the number of isolated methylene units and the number of propylene dyads from the NMR data, at least for the polymers made with the vanadium-based catalyst. The theoretical number of PEP sequences per 100 monomer units is $f_P^2(1 - f_P) \times 100$. This is fairly close to the sum of the sequences of two and three methylene units.

According to Carman and Wilkes,[13] the product of the copolymerization reactivity ratios is given by

$$r_1 r_2 = 1 + f(1 + \chi) - (1 - f)(1 + \chi)^{1/2} \qquad (1)$$

where f = (moles of ethylene)/(moles of propylene) and χ = (% of propylenes in sequences of 2 or greater)/(% of isolated propylenes). They gave an example where f = 0.61, χ = 3.91, and $r_1 r_2$ = 0.405. For the samples in Table II, $r_1 r_2$ is generally in the same range except that for the copolymers from the vanadium-based catalyst, $r_1 r_2$ tends to increase with increasing ethylene/propylene ratio. This means that the tendency toward alternation increases as the level of propylene is increased.

Single Relaxation Time Model. Most viscoelastic relaxations in polymers are characterized by a distribution of relaxation times. This is especially true of secondary or local mode relaxations such as the γ relaxation in polyethylene and other polymers having sequences of four or more methylene units. A relaxation having a single relaxation time would obey the following relationships[14] in terms of the unrelaxed shear modulus at low temperatures and high frequencies, G_u, and the relaxed modulus at high temperatures and low frequencies, G_r.

A complex plane plot of the loss modulus, G'', vs. the storage modulus, G', will be a semicircle centered at $(G_u + G_r)/2$ on the G' axis and having a radius of $(G_u - G_r)/2$. The equation of this curve is

$$\left(G' - \frac{(G_u + G_r)}{2}\right)^2 + (G'')^2 = \left(\frac{G_u - G_r}{2}\right)^2 \qquad (2)$$

The values of G_u and G_r can be computed from the maximum value of G'', and the value of G' at the same temperature and frequency as follows:

$$G_u = G' + G'' \qquad G_r = G' - G'' \qquad (3)$$

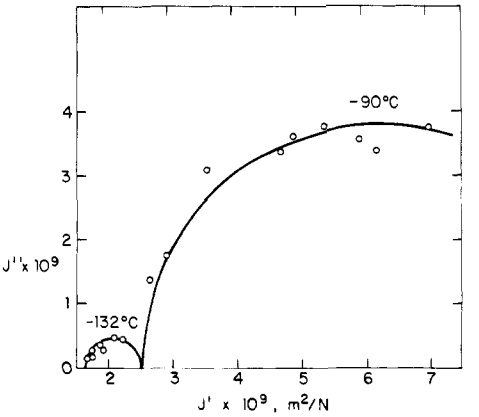

Figure 4. Complex plane plot of compliance for an ethylene/propylene dipolymer of mole ratio 1.3.

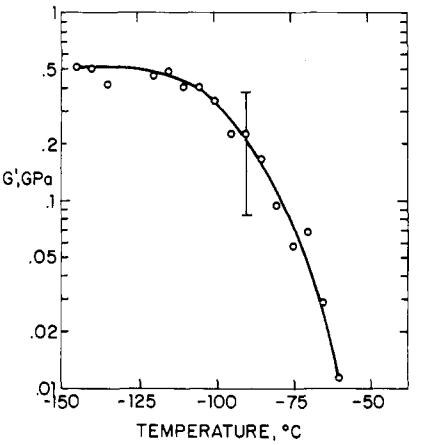

Figure 5. Contribution of a single relaxation time to the softening of sample 1.

Analogous equations can be written in terms of the unrelaxed and relaxed compliances, J_u and J_r. The relationships between the corresponding compliances and moduli are

$$J_u = 1/G_u \qquad J_r = 1/G_r \qquad (4)$$

$$J' = \frac{G'}{(G')^2 + (G'')^2} \qquad J'' = \frac{G''}{(G')^2 + (G'')^2} \qquad (5)$$

The maximum in tan δ or the logarithmic decrement, Δ, does not occur at the same temperature and frequency as the maxima in G'' or J'' but is given by

$$\tan \delta_{max} \cong \frac{\Delta_{max}}{\pi} = \frac{G_u - G_r}{2(G_u G_r)^{1/2}} = \frac{J_r - J_u}{2(J_u J_r)^{1/2}} \qquad (6)$$

Figure 4 is a complex plane presentation of the shear compliance at low temperatures for sample 1. The data are interpreted in terms of two softening processes each characterized by a single relaxation time. The first process, centered at −132 °C, extends from a modulus of 0.6 to 0.4 GPa. This is believed to be a residue of the γ relaxation which is prominent at higher levels of ethylene. The second process, centered at −90 °C, extends from 0.4 to 0.1 GPa.

The torsion modulus of sample 1 is plotted vs. temperature in Figure 5. The vertical bar is located at the temperature of the maximum in G'' and extends to the values of G_u and G_r calculated from eq 3. These values are in reasonable agreement with those from Figure 4 based on the equivalent of eq 2 for the compliance. Finally, the maximum values of Δ_{max} calculated from eq 6 were 2.6 and 2.3 based on the modulus and compliance treatments,

Table III
Spin-Lattice Relaxation Times by Carbon-13 NMR for Sample 1 Dissolved in $CDCl_3$

		T_1, s						
		temp, °C	5	20	30	30	40	54	54
δ	assignt	concn, %	25	25	25	50	25	25	25
19.9	CH_3 EPE		1.04	0.54	1.04	1.14	1.25	2.44	1.54
20.1	CH_3 PPE				0.96	1.11		1.96	1.33
24.8	$S_{\beta\beta}$ $(CH_2)_3$		0.55	0.39	0.50	0.60	0.65	0.84	0.82
27.7	$S_{\beta\delta}$ $(CH_2)_5$		0.85	0.48	0.62	0.60	0.75	1.33	1.05
27.8	$S_{\beta\gamma}$ $(CH_2)_4$		0.56		0.60	0.58	0.69	1.22	1.04
29.9	$S_{\delta^+\delta}$ $(CH_2)_{7+}$		0.97	0.54	0.75	0.71	0.96	1.59	1.23
30.2	$S_{\gamma\delta^+}$ $(CH_2)_{6+}$		0.69	0.54	0.77	0.66	1.01	1.32	1.22
30.0	$S_{\gamma\gamma^+}$, $T_{\beta\gamma^+}$ $(CH_2)_{5+}$		0.94			0.61	1.08	1.59	1.46
33.0	$T_{\delta^+\delta}$		1.03	0.67	0.89	1.01	1.05	2.00	1.60
33.3	$T_{\gamma\delta}$		1.01			0.89	1.24	1.71	1.71
34.5	$S_{\alpha\beta}$ $(CH_2)_2$		0.49	0.46	0.52	0.42	0.58	0.99	0.83
37.3	$S_{\alpha\delta}$ $(CH_2)_4$		0.63	0.32	0.61	0.52	0.75	1.12	0.98
37.6	$S_{\alpha\gamma}$ $(CH_2)_3$		0.64		0.61	0.50	0.82	0.92	1.03
45.8	$S_{\alpha\alpha}$ $(CH_2)_1$			0.37	0.46		0.37		
46.1	$S_{\alpha\alpha}$ $(CH_2)_1$			0.44	0.40		0.50		

respectively. This is in good agreement with the data plotted in Figure 1.

The value of Δ_{max} for the small peak centered at −132 °C in the compliance plot is calculated to be about 0.2. This is obscured by the tail of the larger peaks in Figure 1, but it is similar to the secondary peaks for the samples having higher E/P ratios.

There is thus a good deal of internal evidence that a major portion of the relaxation near −90 °C can be described in terms of a single relaxation time model.

Anisotropic Aspects. The torsion pendulum measures the complex shear modulus, G^*. The Du Pont dynamic mechanical analyzer (DMA)[15,16] operates in flexure and measures the complex Young modulus, E^*. As shown in Figure 6, the large secondary relaxation which is such a prominent feature of the internal friction data obtained with the torsion pendulum is not observed with the DMA. The large peak being absent, the small polyethylene-type γ relaxation peak is revealed. To present the data on a comparable basis, the logarithmic decrement was converted to the loss tangent by the relationship

$$\Delta = \pi \tan \delta \tag{7}$$

The relationship between Young's modulus and the shear modulus is

$$E = 2G(1 + \nu) \tag{8}$$

where ν is Poisson's ratio. If E, G, and ν are all complex quantities, one may write

$$\tfrac{1}{2}(E' + iE'') = (G' + iG'')(1 + \nu' + i\nu'') \tag{9}$$

$$= [G'(1 + \nu') - G''\nu''] + i[G''(1 + \nu') + G'\nu''] \tag{10}$$

If

$$\tan \delta_E = E''/E' \qquad \tan \delta_G = G''/G'$$
$$\tan \delta_\nu = \nu''/(1 + \nu') \tag{11}$$

then

$$\tan \delta_E = \frac{\tan \delta_G + \tan \delta_\nu}{1 - \tan \delta_G \tan \delta_\nu} \tag{12}$$

and

$$\tan \delta_G = \frac{\tan \delta_E - \tan \delta_\nu}{1 + \tan \delta_E \tan \delta_\nu} \tag{13}$$

If

$$\tan \delta_E = 0 \qquad \tan \delta_G = -\tan \delta_\nu \tag{14}$$

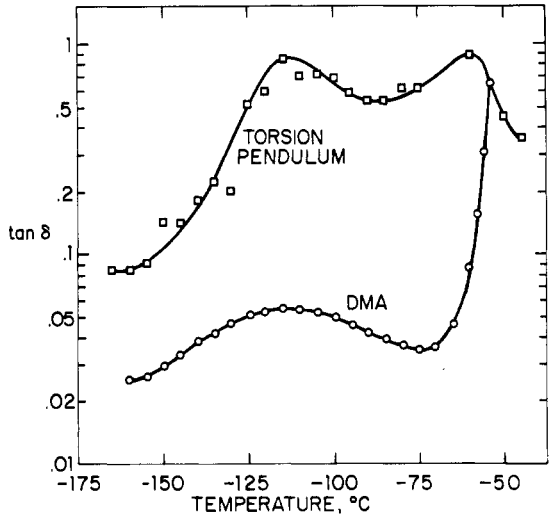

Figure 6. Comparison of tan δ values for sample 1 from the DMA and the torsion pendulum.

Thus a relaxation which is observed in shear but not in tension may be associated with Poisson's ratio which reflects changes in volume on deformation. Perhaps the dilation which occurs in tension forestalls the addition-energy-absorbing process.

The present situation is the opposite of one reported by Barham and Arridge.[17] They found a relaxation at 220 K in high-density polyethylene which was seen in tension but not in shear when the environment was air but not nitrogen, argon, or helium. That relaxation was tentatively assigned to cyclic adsorption and desorption of carbon dioxide. In that instance, it follows from eq 12 that

$$\tan \delta_G = 0 \qquad \tan \delta_E = \tan \delta_\nu \tag{15}$$

Other Observations by Nuclear Magnetic Resonance. Spin–lattice relaxation times were measured by proton NMR for samples 1 and 5, and the data are plotted in Figure 7. A Bruker SXP 100 spectrometer was used at a frequency of 90 MHz, and the H_1 field was 11.7 G. The frequency in the spin-locking field for the $T_{1\rho}$ experiments was 50 kHz. Minima corresponding to T_g were observed near 45 °C for T_1 and −25 °C for $T_{1\rho}$. A secondary minimum near −110 °C for T_1 and below −145 °C for $T_{1\rho}$ has been assigned to the rotation of methyl groups in a number of closely related hydrocarbon polymers.[18-20] While the large secondary relaxation is not reflected in a corresponding minimum in T_1 or $T_{1\rho}$, these relaxation times are shorter in sample 1 at all temperatures below T_g.

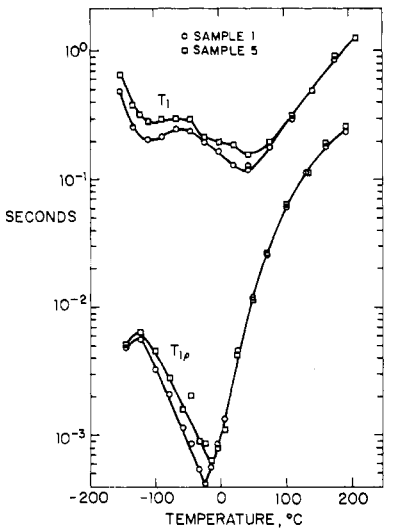

Figure 7. Spin–lattice relaxation times by proton NMR.

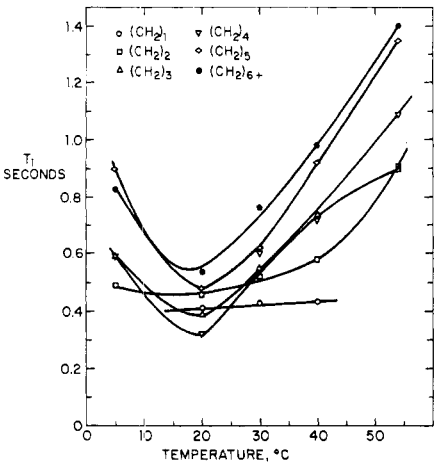

Figure 8. Spin–lattice relaxation times by carbon-13 NMR for various segments in sample 1.

Above T_g, the two polymers have virtually the same relaxation times. This may be analogous to the situation in poly(vinyl acetate), where the effect of the ester group relaxation on T_1 and $T_{1\rho}$ is very subtle.[18]

Measurements of T_1 were also made by carbon-13 NMR on sample 1 for each type of carbon detected. An inversion–recovery procedure was used, and the pulse sequence was $(180°\text{–}t\text{–}90°\text{–}T)_n$. T was about 5 s (3–5 times the longest T_1), and t varied from 0.01 to 3.2 s. These measurements were done on 25 or 50% solutions in $CDCl_3$. The carbons are primary (CH_3), secondary (CH_2), or tertiary (CH). They are also identified in terms of their relationships to branch points in each direction along the chain. Thus, $S_{\alpha\alpha}$ is an isolated methylene in a sequence of propylene units, and $S_{\alpha\beta}$ is in a dimethylene link associated with a propylene reversal. $S_{\alpha\gamma}$ and $S_{\beta\beta}$ are part of $(CH_2)_3$ links, $S_{\alpha\delta}$ and $S_{\beta\gamma}$ are in $(CH_2)_4$, and $S_{\gamma\gamma}$ and $S_{\beta\delta}$ are in $(CH_2)_5$ sequences.

The data are presented in Table III. For most carbons, there is a fairly sharp minimum near 20 °C. However, for the $S_{\alpha\alpha}$ and $S_{\alpha\beta}$ carbons, T_1 is almost independent of temperature in this region. The average relaxation times for the carbons in various polymethylene sequences are plotted in Figure 8. The dependence of T_1 on temperature increases with the length of polymethylene sequences up to about five. For the longer sequences, the activation energy calculated from the slope of ln T_1 vs. reciprocal absolute temperature is 5–6 kcal/mol for both carbon-13 and proton data.

Even in the presence of the solvent, the relaxation of short polymethylene sequences differs from that of longer sequences. Clearly, intrachain factors play a major part in the internal motions of this polymer.

Acknowledgment. Thanks are due to A. L. Moore, A. Su, and R. C. Thamm for experimental copolymer samples and to E. G. Brame, D. W. Ovenall, A. D. English, and A. J. Vega for NMR measurements.

References and Notes

(1) P. Manaresi and V. Giannella, *J. Appl. Polym. Sci.*, **4**, 251 (1960).
(2) E. G. Kontos and W. P. Slichter, *J. Polym. Sci.*, **61**, 61 (1962).
(3) J. J. Mauer, *Rubber Chem. Technol.*, **38**, 979 (1965).
(4) C. A. F. Tuijnman, *J. Polym. Sci., Part C*, **No. 16**, 2379 (1967).
(5) Y. V. Selenev and G. M. Bartcnev, *Plaste Kautsch.*, **17**, 731 (1970).
(6) E. P. Baldwin and G. Ver Strate, *Rubber Chem. Technol.*, **45**, 709 (1972).
(7) R. F. Boyer, *Macromolecules*, **6**, 288 (1973).
(8) C. J. Carman, R. A. Harrington, and C. E. Wilkes, *Macromolecules*, **10**, 536 (1977).
(9) J. C. Randall, *Macromolecules*, **11**, 33 (1978).
(10) A. H. Willbourn, *Trans. Faraday Soc.*, **54**, 717 (1958).
(11) E. G. Brame and H. E. Holmquist, *Rubber Chem. Technol.*, **52**, 1 (1979).
(12) G. J. Ray, P. E. Johnson, and J. R. Knox, *Macromolecules*, **10**, 773 (1977).
(13) C. J. Carman and C. E. Wilkes, *Rubber Chem. Technol.*, **44**, 781 (1971).
(14) N. G. McCrum, B. E. Read, and G. Williams, "Anelastic and Dielectric Effects in Polymeric Solids", Wiley, New York, 1967.
(15) R. L. Blaine and L. Woo, *Polym. Prepr., Am. Chem. Soc., Div. Polym. Chem.*, **17** (2), 1 (1976).
(16) R. M. Ikeda and H. W. Starkweather, *Polym. Eng. Sci.*, **20**, 321 (1980).
(17) P. J. Barham and R. G. C. Arridge, *Polymer*, **20**, 509 (1979).
(18) D. W. McCall, *Acc. Chem. Res.*, **4**, 223 (1971).
(19) W. P. Slichter, NMR. *1971*, **4**, 209 (1971).
(20) V. J. McBriety, *J. Chem. Soc., Faraday Trans. 2*, **68**, 105 (1972).